Design and Performance of Capping Layers for EUV Multilayer Mirrors

S. Bajt, H. N. Chapman, N. Nuygen, J. Alameda, J. C. Robinson, M. Malinowski, E. Gullikson, A. Aquila, C. Tarrio, S. Grantham

This article was submitted to
28th Annual International Symposium on Microlithography, Santa Clara, Ca, February 23-27, 2003

U.S. Department of Energy

March 10, 2003

Lawrence
Livermore
National
Laboratory

DISCLAIMER

Design and performance of capping layers for EUV multilayer mirrors

Sasa Bajt[*a], Henry N. Chapman[a], Nhan Nuygen[a], Jennifer Alameda[a], Jeffrey C. Robinson[a],
Michael Malinowski[b], Eric Gullikson[c], Andy Aquila[c], Charles Tarrio[d], Steven Grantham[d]

[a]Lawrence Livermore National Laboratory, 7000 East Avenue, Livermore, CA 94550, USA;
[b]Sandia National Laboratories, 7011 East Avenue, Livermore, CA 94550, USA;
[c]Lawrence Berkeley National Laboratory, CXRO, Berkeley, CA 94720, USA;
[d]National Institute of Standards and Technology, Gaithersburgh, MD 20899, USA

ABSTRACT

The reflectance stability of multilayer coatings for extreme ultraviolet lithography (EUVL) in a commercial tool environment is of uttermost importance to ensure continuous exposures with minimum maintenance cost. We have made substantial progress in designing the protective capping layer coatings, understanding their performance and estimating their lifetimes based on accelerated electron beam and EUV exposure studies. Our current capping layer coatings have about 40 times longer lifetimes than Si-capped multilayer optics. Nevertheless, the lifetime of current Ru-capped multilayers is too short to satisfy commercial tool requirements and further improvements are essential.

Keywords: Extreme ultraviolet (EUV) lithography, multilayers, optics, capping layer, ruthenium, oxidation resistance, reflectivity

1. INTRODUCTION

The next generation extreme ultraviolet lithography (EUVL) is based on Mo-Si coated reflective optics optimized for 13.5 nm wavelength. Recent high-quality Mo-Si multilayers have been made using DC magnetron sputtering[1] RF magnetron sputtering[2], ion beam sputtering[3], electron beam evaporation with ion beam polishing[4], pulsed laser deposition[5] and rotary magnetron sputtering[6]. However, the highest reported reflectivities are achieved with DC magnetron sputtering[7-8] using interface-engineered multilayers in which the Mo and the Si layers are separated with thin layers of low Z materials such as B_4C or C. The reflectivity of multilayer coatings is of great importance because the optical throughput of the EUVL tools is proportional to:

$$\int R^n(\lambda)d\lambda$$

where R is the reflectance of the multilayer and n is the number of reflective mirrors in the EUVL tool. For commercial EUVL optical trains *n* is typically 9 or higher and even a small change in reflectivity of about 1% will lead to a noticeable change in the throughput of such a system. It is believed that an EUVL tool should be able to expose 100 to 120, 300mm wafers/hr to be commercially viable. A breakthrough in source development is needed but improvements in multilayer reflectivity will make this goal more feasible. However, in addition to the essential high reflectivity the multilayers must maintain their performance over a reasonably long operating lifetime. The lifetime of multilayers is currently one of the highest risks for EUVL commercial viability. Mo-Si multilayers have traditionally been terminated with a Si layer, which forms a thin and stable oxide in the air. For an ideal multilayer it would be better to terminate the multilayer with molybdenum absorber layer. However, it was shown early on that molybdenum is not stable in the air[9]. Early studies of the silicon-capped multilayer lifetimes[10] were done in a good vacuum of <5 x 10^{-8} mbar. Based on the results from EUV exposures under these conditions it was extrapolated that a yearly dose will not significantly alter the

---

performance of x-ray optics if the optics is maintained in high vacuum conditions. We have found, however, that for multilayers in the environments of commercial tools, these estimates are overly optimistic.

The optical systems of EUV lithographic tools will operate in unbaked vacuum systems[11]. Therefore, it is crucial that lifetime tests of multilayers are performed in relevant environments, where the main contaminants are water vapor and hydrocarbons[12-14]. Ideally the tests should be performed by exposing the multilayers with the EUV source planned to be used in the commercial tools. Because the sources are still being developed, and there is a limited amount of time available for these experiments on high brightness synchrotron beamlines, the experiments are often performed with electron beams[1, 15]. It has been demonstrated that molecular contamination is caused by EUV induced secondary electrons. Electron-beam exposure experiments are tailored to give a similar energy distribution of secondary electrons and depth penetration as the EUV exposures to attempt to cause the same amount of damage, however, there is still much unknown about the relationship between the EUV- and electron beam-induced damage. A recent study focused on oxidation caused by EUV- and electron-beam exposure of Si-capped multilayers [16]. The oxidation mechanism is likely very different for different material and this paper presents the results of EUV- and electron beam-induced oxidation on Si- and Ru-capped multilayers under one particular environmental condition.

The main contamination for projection optics is carbon deposition and oxidation. Condenser optics are exposed to quite different environment to the projection optics and require different solutions for lifetime improvements[17]. For example, the first condenser optic, which collects light from the plasma source usually has a direct line of sight to the plasma and is susceptible to sputtering, implantation, carbon deposition, oxidation and debris contamination. In general, the condenser optics are also exposed to a broader spectrum and higher heat load than the projection optics and require active cooling in order to minimize thermal induced multilayer effects such as wavelength shift and reflectance loss. Fortunately, the specifications for condenser optics are less stringent and possible solutions include economic, replaceable substrates and removable coatings[18].

The topic of this paper is the lifetime of projection optics. The projection optics have very stringent requirements for fabrication, multilayer deposition, and alignment and must have lifetimes of at least 5 years. We define the lifetime as the time in which each individual projection optic is allowed to lose up to 1.6% (absolute) in reflectance. The lifetime of projection optics is limited by two effects: carbon deposition and oxidation. It has been demonstrated that carbon can be removed, for example, by using RF oxygen, RF hydrogen[19], atomic hydrogen[20] and ozone[12, 14] with only a minor degradation of mutilayer reflectivity. Avoiding carbon deposition is an even better solution. This idea was proposed by Klebanoff et al.[13] who showed that carbon deposition is substantially reduced in an environment where there is a mixture of water vapor and ethanol. Oxidation is more problematic because once an oxide is formed it can not be removed. Oxides also strongly absorb EUV light and for example, a small increase of 1.5 nm in oxide layer is sufficient to decrease reflectance by 1.6% (absolute), the lifetime budget for projection optics. Oxidation resistant capping layers are essential to increase EUV multilayer lifetimes.

Different capping layer materials have been proposed to be used on Mo-Si multilayers based on their optical constants[21]. However, in addition to optical properties, capping materials need to meet other criteria to be good candidates for oxidation resistant materials. The material has to form a continuous layer for thickness of few nm, it has to form a sharp, smooth interface with the material underneath and has to be oxidation resistant in water vapor environment. Unfortunately, the data about EUV induced oxidation in the presence of water vapor is very scarce. Most of the data have been collected only recently on Si-capped Mo-Si multilayers[14, 16]. Initial results on promising oxidation resistant capping layers include Ru-[7] and C-layers[22].

2. EXPERIMENTAL METHODS

2.1 Deposition System and Sputtering Rate Calibration

Multilayers were deposited using a DC-magnetron sputtering system described previously by Bajt et al.[7]. In this system in which the substrates are rotated on a platter above a circular arrangement of targets, two of the sputtering guns, placed 180 degrees apart, are rectangular (12.7 x 25.4 cm), and two are circular (10 cm). This geometry places each sputtering

gun into its own quadrant. The two large sputtering guns are used to sputter Mo and Si, while the small sputtering guns are used to sputter B_4C (for interfacial barriers) and Ru, respectively. The sputtering guns, which are mounted on the bottom of the deposition chamber, are facing up, while the substrates, mounted on the rotating platter are facing down. Using this setup, up to two substrates with different multilayer design can be coated per deposition run. The substrates, which spin during the deposition, are usually super-polished Si (100) wafers. Most of the coatings for this study were done on 100 mm diameter substrates. The platter with affixed substrate spinners rotates over the sputtering targets during the deposition and the platter rotational velocity controls the individual layer thickness. The deposition runs for this study were done at 1 mTorr of ultrahigh-purity Ar gas with a chamber base pressure of 2×10^{-7} Torr or better. Applied powers of 360W on Si, 170W on Mo, 100W on B_4C and 50W on Ru targets were used, respectively.

The sputtering rates of the Mo and Si targets were calibrated by depositing multilayes in which the velocity of the platter was varied over the sources at constant power, and subsequently determining the Mo/Si multilayer periods by fitting the Bragg peaks in the small angle x-ray diffraction spectra in the variable-period multilayers. The sputtering rates of B_4C and Ru were determined from single films coated at constant power. Small angle X-ray diffraction measurements were performed with a Rigaku DMAX-IIB diffractometer with a Cu K_ rotating anode source ($\lambda = 0.154$ nm).

2.2 EUV Reflectometry

The synchrotron-based reflectometer at beamline 6.3.2. at the Advanced Light Source (ALS, Lawrence Berkeley National Laboratory) is ideally suited for characterization of multilayer coated optics and was used to measure the reflectance of our multilayers. This reflectometer has high stability, high spectral purity, and small beam diameter[23]. This reflectometer can routinely achieve a wavelength precision of 0.002 nm and reflectance repeatability of ±0.2%. Beamline software allows collection of individual reflectance spectra, line scanning or 2D mapping.

2.3 Atomic Force Microscopy (AFM)

The surface roughness of the multilayers was characterized using a Digital Instruments Dimension 3000 Atomic force microscope (AFM), operating in tapping mode. The AFM is fitted with a Nanoscope IIIA Controller, a phase extender box and standard Si tip. The surface roughness was measured on each sample over an area of 2 x 2 _m.

2.4 Auger Electron Spectroscopy (AES)

Auger electron spectroscopy was used to identify the elemental composition of the multilayers. An ion beam sputter source was used to remove less than one monolayer of material from the surface at a time during continued monitoring of Auger electron spectra to determine the composition and chemistry of the exposed surface. A PHI660 scanning Auger microprobe was operated at 5 keV and 75 nA, and the beam was rastered over a 50 x 50 _m area at 30° from normal incidence. A PHI Duoplasmatron ion source was operated at 2 keV and 8 nA current at a 45° angle. Sputtering rates of Mo and Si within the multilayer were calibrated using the known multilayer period, which was determined by small angle x-ray diffraction or EUV reflectometery. No attempt was made to adjust sputtering rates for the Ru and B_4C capping layers.

2.5 X-ray Photoelectron Spectroscopy (XPS)

Additional compositional information of the multilayers was obtained by XPS. The XPS data were collected using a Quantum 2000 scanning XRS system with a focused monochromatic Al K_ x-ray (1486.7 eV) source of excitation and a spherical section analyzer. The instrument has a 16-element multichannel detection system. A 200 _m diameter x-ray beam was used for analysis. The x-ray beam was incident normal to the sample and the electron detector was at 45° away from normal. The pass energy was 23.5 eV giving overall energy resolution of 0.3 eV. The collected data were referenced to an energy scale with binding energies for Cu $2p_{3/2}$ at 932.72±0.05 eV and Au $4f_{7/2}$ at 84.01±0.05 eV. Binding energies were also referenced to the C1s photoelectron line arising from adventitious carbon at 284.6 eV. Low energy electrons and argon ions were used for specimen neutralization.

2.6 Electron Beam Exposures

Electron beam exposures were performed in a carbon system at Sandia National Laboratories in Livermore (see Figure 1). The system consists of two small, differentially pumped chambers. This is necessary in order to simultaneously have the electron beam gun in a good vacuum (10^{-9} Torr) for stable operation and the sample in an oxidizing environment ($10^{-7} - 10^{-6}$ Torr H_2O partial pressure). Electrons with 1 keV energy and 500 _A/cm^2 current density were used in this study. The beam area on the sample was estimated to be about 2 mm^2. The sample chamber can accommodate one small sample (~2.5 x 1.25 cm) and a phosphorous screen. The phosphorous screen was used to check the shape, size and position of the electron beam on the sample. A variable leak valve with an attached high purity H_2O cylinder was used to adjust H_2O partial pressure in the sample chamber and a Residual Gas Analyzer (RGA) monitored the quantity of water and other impurities in the chamber. The pressure and the secondary electron yield were recorded as a function of time during the exposures. The secondary electron yield (SEY) emission is defined as a ratio of the secondary electron current to the primary electron current. The primary electron current is measured by applying a 100 V bias on the sample while the secondary electron beam current is derived from the difference between the currents of the sample with an without bias applied. The beam current was stable within ±20% for daylong exposures.

2.7 Extreme Ultraviolet (EUV) Exposures

Two samples in this study were exposed to EUV radiation in an oxidizing environment. The experiments were performed at the National Institute of Standards using a multilayer exposure beamline at SURF. A 75 mm diameter, 1.5 m radius multilayer coated spherical mirror positioned approximately 4 m from the tangent point of the electron beam in the ring reflects. with a deviation of 20°. A 0.2 _m thick, mesh-backed Be foil provides both filtering of long wavelength radiation and vacuum isolation between the exposure chamber and the mirror chamber, which must be kept at a background pressure of <20x10^{-8} Torr (Figure 2). The light is incident on the sample at an angle of 10° from normal. Incident and reflected radiation intensity are measured using a Zr/C coated photodiode. The photoemission from the sample surface was monitored. For these measurements, a stainless steel aperture biased at 100 V, offset 5 mm from the sample surface, was used. The exposures were performed using ~800 mW/cm2 current density in 2x10^{-6} Torr of H_2O vapor pressure. Accumulated 60-hours exposures were done within one week using five 12 hour shifts separated with five 12 hours of shutdown.

3. RESULTS AND DISCUSSION

In an earlier paper[7] we reported about promising initial results of ruthenium as an oxidation resistant capping layer. In that study ruthenium was deposited either on the top of a Si layer, on the top of a Mo layer or on the top of a B_4C layer. We found that Ru deposited directly on the top of a Si layer inter-diffused with Si and formed ruthenium silicide. When exposed to the electron beam in the presence of water vapor this particular capping layer did not perform well. The main disadvantage of Ru deposited on a Mo layer was that this results in a low reflectivity of 62%. Both Ru and Mo are absorbers and form too thick an absorber layer for the constructive interference with the multilayer underneath. Higher reflectivity (~66%) Ru-capped multilayers were achieved with a 0.6-0.8 nm thick Ru layer deposited on the top of a 1.3 nm thick Mo layer. However, the multilayers with such thin Ru layers have not been studied for their lifetime stability.

The study described in this paper was focused on the design and performance of capping layers for EUV multilayers. Capping layers were deposited directly on the top of standard Mo/Si multilayers (starting with Si at the substrate and ending with Mo) with 40 bilayers unless otherwise specified. The capping layer in this study consists of three sub-layers: Ru-on-B_4C-on-Si, as shown in Figure 3. The main purpose of the B_4C layer is to prevent interdiffusion of Si and Ru and to create a sharp Ru-on-B_4C interface. The typical initial reflectance of Ru-capped multilayers was 65.5 ± 0.5 % at 13.3 nm at 5° off normal incidence, with a 5.5 nm peak width (Figure 4). Aging of the multilayer in air (i.e. with no EUV exposure) showed no measurable reflectance loss after six months. Each sample was characterized before and after the exposures for reflectance as a function of wavelength, for surface roughness, for surface chemistry and bonding and for chemical depth profiles using the techniques described in section 2. In addition, secondary electron yield (SEY) emission was collected during the exposures.

3.1 Electron beam exposures

Ru and Si-capped multilayers were exposed to the electron beam in the presence of water vapor, as described in Section 2.6. We will first describe the results of a Ru-capped multilayer that was exposed to the electron beam for 360 hours. The water vapor pressure, which was kept constant, was 2×10^{-6} Torr. The partial pressure of other contaminants was $<10^{-8}$ Torr. Results from this long exposure on the Ru-capped multilayer are presented in Figure 5. Figure 5, in which the SEY is plotted as a function of exposure time, shows a dramatic change in SEY emission occurring between 50 and 100 hours of exposure. Furthermore, the reflectivity drop as a function of exposure time is strongly correlated with the changes in SEY emission (Figure 6). The reflectance loss in the first 50-60 hours (~ 2%, absolute) is of most interest because this is greater than the maximum allowable reflectivity loss for commercial tool mirrors. However, to better understand the oxidation mechanisms we continued the exposures well beyond 60 hours. As shown in Figure 5, the initial 2% reflectivity drop within the first 60 hours of exposure, is followed with a huge reflectivity drop of 17% over the next 50 hours of exposure and another 2% reflectivity drop for the next 250 hours of exposure. Hence, for a fixed current density and water vapor pressure, the reflectivity loss rate is not linear with time and furthermore seems to be very material dependent. High frequency surface roughness was characterized with AFM as described in Section 2.3. The typical surface roughness of Ru-capped multilayers is 0.18-0.19 nm rms on as-deposited samples and in the areas that have not been exposed to the electron beam. However, in the areas that were exposed to the electron beam in the presence of water vapor we measured substantial increase in surface roughness, as shown in Figure 6. For example, surface roughness in an area exposed for 60 hours increased to 1.19 nm rms and for 100 hours exposure it increased to 2.87 nm rms. However, for an area exposed for a 200 hours the surface roughness became smoother (1.65 nm rms) again. Interestingly, the sample exposed to the electron beam with only 10^{-8} Torr water vapor pressure in the system shows no measurable reflectance drop after 170 hours of exposure and no change in surface roughness. This clearly demonstrates the importance of keeping the water vapor level as low as possible in the system in order to increase the x-ray optics lifetime.

Using the XPS technique, detailed in Section 2. 5., we compared the surface chemistry of unexposed Ru-capped sample and Ru-capped sample that has been exposed to the electron beam and water vapor for ~100 hours. The results are shown in Figure 7. While the unexposed area shows a slightly oxidized Ru capping layer with traces of C and N, we could easily detect Mo, Si and higher concentrations of C and O in the exposed area. High-resolution core-level spectra of O 1s, B 1s, Ru 3d + C1s, Mo 3d and Si 2p for different exposure times indicate that –OH, O and/or H reach the B_4C layer within the first 60 hours of exposure, and change the chemical state (bonding) of the B_4C. Boron is undetectable in spots which were exposed to 100 hours or longer. We confirmed this with Auger depth profiles that show trace amounts of B and C on the surface but no defined layer of B_4C underneath the Ru layer. XPS data also show a sudden increase in oxidation of Mo and Si layer between 60 and 100 hours of exposure. Interestingly, this matches the large change in SEY emission, increase in the surface roughness and decrease in reflectivity. Our hypothesis is that B forms volatile species with –OH or H and escapes the multilayer. It is likely that the oxidation is initiated at voids and pinholes in the Ru layer. When Ru oxidizes it expands, and perturbs the surface. This causes increased surface roughness and brings Si and Mo closer to the surface. This might explain the detection of Si and Mo at the surface with XPS.

Comparing the electron beam exposure results of Ru- and Si-capped multilayers, we find that the lifetime of Ru-capped multilayers is greater than of Si-capped. Both multilayers were exposed under the same conditions as described above. After 60 hour exposures we mapped the samples reflectivities at the peak wavelength using the reflectometer. The reflectivity as a function of wavelength was then measured in the center of the exposed area. The reflectance maps are show in Figure 8. The reflectivity of the exposed Si-capped multilayer dropped in the center of the exposed area by 17%, while the reflectivity of exposed Ru-capped multilayer dropped in the center by only 2%. There was no measurable change in the wavelength for either multilayer, confirming that the oxidation affected only the surface area. From the electron beam exposure tests we find that for the Ru-capped multilayer a reflectivity drop of 1.6% (corresponding to our criterion for failure) occurred after and exposure of 30 ± 5 hours at a current density of 500 $\mu A/cm^2$. From previous experiments[24] we determined the relationship between the current of the secondary electrons and the EUV power, to be 1 μA of electron beam corresponds to 3 mW of EUV exposure. Using this conversion factor, the dose for failure is therefore D^e_F = 500 $\mu A/cm^2$ x 3 mW/μA x 30± 5 hours = 1.62 x 10^5 J/cm^2 for the Ru-capped multilayers.

3.2 EUV exposures

To verify the validity of the electron beam exposures we tested the oxidation resistance of Ru- and Si-capped multilayes also with EUV light in the presence of water vapor. Additionally, the plasma source operates as a pulsed source. In contrast, EUV light from a synchrotron source has a very narrow bandwidth and synchrotron is effectively a continuous source.

The 60-hour EUV exposures were performed with an average current density of 800 mW/cm² in a chamber with 2 x 10⁻⁶ Torr of water vapor pressure as described in Section 2.7. Again, Ru- and Si-capped multilayers were exposed under identical conditions and the results are shown in Figure 9. The Ru-capped multilayer experienced a reflectivity drop of 1.5% while the Si-capped multilayer showed a reflectivity drop of 16.4%. The surface roughness of Ru-capped multilayer increased from 0.19 nm rms to 0.62 nm rms. This is a similar surface roughness increase observed on the electron beam exposed sample that experienced a similar reflectance drop. The surface roughness of as-deposited Si-capped multilayers is typically 0.15-0.18 nm. The Si-capped EUV exposed spot still has a smooth surface (0.25 nm rms) but the reflectivity dropped by 17%. The oxidation in Si-capped multilayers is not limited to the surface layer but had to change few more layers underneath in order to explain such a large reflectivity drop. These results imply that electrons and EUV exposures are similar. The exposure time at which the reflectivity dropped by 1.6% was 60 ± 2 hours. Thus, the dose for failure is $D^{EUV}_F = 800$ mW/cm² x 60 ± 2 hours = 1.73 x 10⁵ J/cm².

3.3 Lifetime calculations

The lifetime of the optical elements of an EUV projection imaging system depends on the power density on each of those elements during exposure. This, in turn, depends on the area of the optics, which will be specific to an optical design, on the reflectivity of the mirrors, and on the wafer throughput of the system. We chose for this study a six-mirror 0.25 NA ring-field optic that has been published[25], referred here as the Advanced Optical Package (AOP). The areas of the kidney-shaped clear apertures of each of the mirrors of this design are given in Table 1. To calculate the power densities at the mirrors, we assume that the mask pattern being printed is detailed, with a large variation in pattern shapes and sizes, so that the diffracted (ie all reflected) intensity from the mask uniformly illuminates the clear apertures of the mirrors. Furthermore, we assume that all the light diffracted from the mask remains within the acceptance numerical aperture (and acceptance field) of the optical system. We first compute the power required at the wafer to expose at a rate of a particular number of wafers per hour, and then work backwards through the system, to find the power required to be reflected from each mirror. The power at the wafer is simply given by the required dose to print[26], D_w, taken here to be 5 mJ/cm², multiplied by the printed area, A_w. For a 300-mm diameter wafer, this area is 707 cm². Each wafer must be printed in a time t_w (we take $t_w = 36$ s for 80 wafers/hour with a 20% overhead), which gives a required power incident on the wafer of $P_w = D_w A_w / t_w$. With the values given above, the required power is 98.2 mW. With a mirror reflectance of R, the incident power on that mirror is $1/R$ of the reflected power, and the power absorbed in the mirror is $(1-R)/R$ of the reflected power. Therefore, the power absorbed by the nth mirror in the six-mirror system is $P_w (1 - R)/R^{7-n}$. Since the mirror lifetime measurements are characterized by incident power, we compute the power incident on the nth mirror as $P_n = P_w / R^{7-n}$. Note that we need not make any assumption in the way the wafer is exposed, nor do we need to know the area of the image field of the optic. All that is needed for the calculation is that the wafer must be patterned over a certain area, in a certain time, with a certain dose. All the photons that expose the wafer must have passed through the optical system within the same time required to expose the wafer.

Given an area A_n of the clear aperture of mirror n we now see that the power density incident on that mirror is given by

$$J_n = P_n / A_n = P_w / (A_n R^{7-n}) = D_w A_w / (t_w A_n R^{7-n}),$$

which can obviously be generalized to systems with other than six mirrors. The power densities of the mirrors of the AOP are given in Table 1, and it is seen for this particular design that mirror M1 receives the highest power density. Note that the equation is valid for the mask, for $n = 0$ and A_n set equal to the patterned area of the mask. We then compute mirror lifetimes from our experimentally determined dose for failure, D_F, which was found from the exposure time to fail (failure is taken to be a reduction in reflectivity of 1.6%) multiplied by the equivalent EUV power density.

As shown in Sections 3.1 and 3.2, we have $D^e_F = 1.62 \times 10^5$ J/cm^2 from the electron-beam exposures and $D^{EUV}_F = 1.73 \times 10^5$ J/cm^2 from the accelerated EUV exposures. That is, the lifetime of mirror n, in seconds, is $L_n = D_F/(0.8 J_n)$. Here we have accounted for the 20% overhead time of exposure. The lifetimes of the optics of the AOP design are given in Table 1, for the two estimates of D_F. For the highest dosed mirror, M1, the lifetime is based on electron beam extrapolation is 0.4 years and the lifetime based on EUV extrapolation is 0.3 years.

4. SUMMARY

A new capping layer design consisting of Ru-on-B4C-on-Si layer has been tested with accelerated electron beam and EUV light in water vapor environment. The results were compared with the results from standard Si-capped multilayer that were exposed under identical conditions. Lifetime calculations show that the 1.6% reflectance loss on Si-capped multilayers occurs within a week to a few months. Ru-capped multilayers have about 40x longer lifetime under identical conditions. Hence, the lifetime of Ru-capped multilayers is estimated to be 3 months to many years.
The results from electron beam exposures and EUV exposures are remarkably similar. This validates electron beam exposure experiments. Long electron beam exposures are more feasible because they do not require synchrotron source.
The Ru-capping layer is superior to Si-capping layer. However, the lifetime of Ru-capped multilayers on most mirrors still does not meet stringent commercial tool specifications. Improvements to existing Ru capping layer and new approaches to robust capping layer must be developed.

5. ACKNOWLEDGMENTS

6. REFERENCES

1. J. A. Folta, S. Bajt, T. W. Barbee Jr., R. F. Grabner, P. B. Mirkarimi, T. Nguyen, M. A. Schmidt, E. Spiller, C. C. Walton, M. Wedowski, and C. Montcalm, Advanced in multilayer reflective coatings for extreme-ultraviolet lithography, SPIE **3676**, 702-709 (1999).
2. M. Putero-Vuaroqueaux and B. Vidal, Extreme-ultraviolet multilayer mirrors deposited using radio-frequency-magnetron sputtering: the influence of self-bias voltage on reflectivity and roughness, *J. Phys.: Condens. Matter* **13**, 3969-3976 (2001).
3. E. Spiller, S. Baker, P. A. Mirkarimi, V. Sperry, E. Gullikson, and D. Stearns, High performance Mo/Si multilayer coatings for EUV lithography using ion beam deposition, submitted to Appl. Opt. (2003).
4. E. Louis, A. E. Yakshin, P. C. Görts, S. Oestreich, R. Stuik, E. L. G. Maas, M. J. H. Kessels, Bijkerk, M. Haidl, S. Müllender, M. Mertin, D. Schmitz, F. Scolze and G. Ulm, Progress in Mo/Si multilayer coating technology for EUVL optics, SPIE **3997**, 406-411 (2000).
5. St. Braun, R. Dietsch, M. Haidl, Th. Holz, H. Mai, S. Müllender, R. Scholz, Mo/Si –multlayers for EUV applications prepared by pulsed laser deposition (PLD), *Microelectr. Eng.* **57-58**, 9-15 (2001).
6. M. Shiraishi, N. Kandaka, K. Murakami, Mo/Si multilayers deposited by low-pressure rotary magnet cathode sputtering for extreme ultraviolet lithography, in this SPIE Proc.
7. S. Bajt, J. Alameda, T. Barbee Jr., W. M. Clift, J. A. Folta, B. Kaufmann, E. A. Spiller, Improved reflectance and stability of Mo-Si multilayers, *Opt. Eng.* **41**, 1797-1804 (2002).
8. St. Braun, H. Mai, M. Moss, R. Scholz and A. Leson, Mo/Si multilayers with different barrier layers for applications as extreme ultraviolet mirrors, *Jpn. J. Appl. Phys.* **41**, 4074-4081 (2002).
9. J. H. Underwood, E. M. Gullikson, and K. Nguyen, Tarnishing of Mo/Si multilayer x-ray mirrors, *Appl. Opt.* **32**, 6985-6990 (1993).

10. D. P. Gaines, R. C. Spitzer, N. M. Ceglio, M. Krumrey, and G. Ulm, Radiation hardness of molybdenum silicon multilayers designed for use in a soft-x-ray projection lithography system, *Appl. Opt.* **32**, 6991-6998 (1993).

11. L. E. Klebanoff, M. E. Malinowski, P. Grunow, W. M. Clift, C. Steinhaus, A. H. Leung, S. J. Haney, First environmental data from the EUV engineering test stand, SPIE **4343**, 342-346 (2001).

12. M. Wedowski, S. Bajt, J. A. Folta, E. M. Gullikson, U. Kleineberg, L. E. Klebanoff, M. E. Malinowski, W. M. Clift, Lifetime studies of Mo/Si and Mo/Be multilayer coatings for extreme ultraviolet lithography, SPIE **3767**, 217-224 (1999).

13. L. E. Klebanoff, W. M. Clift, M. E. Malinowski, C. Steinhaus, P. Grunow, and S. Bajt, Radiation-induced protective carbon coating for extreme ultraviolet optics, *J. Vac. Sci. Technol.* **B 20**, 696-703 (2002).

14. S. Oestreich, R. Klein, F. Scholze, J. Jonkers, E. Louis, A. Yakshin, P. Görts, G. Ulm, M. Haidl, and F. Bijkerk, Multilayer reflectance during exposure to EUV radiation, SPIE **4146**, 64-71 (2000).

15. N. Koster, B. Mertens, R. Jansen, A. van de Runstraat, F. Stietz, M. Wedowski, H. Meiling, R. Klein, A. Gottwald, F. Scholze, M. Visser, R. Kurt, P. Zalm, E. Louis, A, Yakshin, Molecular contamination mitigation in EUVL by environmental control, *Microelect. Eng.* **61-62**, 65-76 (2002).

16. M. E. Malinowski, C. A. Steinhaus, D. E. Meeker, W. M. Clift, L. E. Klebanoff, S. Bajt, Relation between electron- and photon-caused oxidation in EUVL optics, this SPIE Proc. (2003).

17. L. E. Klebanoff, P. A. Grunow, S. Graham, W. M. Clift, A. H. Leung, S. J. Haney, Environmental data from the Engineering Test Stand, SPIE **4688**, 310-315 (2002).

18. E. Spiller, http://cletus.phys.columbia.edu/pxrms/, conference presentation at PXRMS'02, Chamonix Mont Blanc, France, 2002.

19. S. Graham, C. Steinhaus, M. Clift, L. Klebanoff, Radio-frequency discharge cleaning of silicon-capped Mo/Si multilayer extreme ultraviolet optics, *J. Vac. Sci. Technol.* **B 20**, 2393-2400 (2002).

20. S. Graham, C. E. Steinhaus, M. Clift, L. E. Klebanoff, S. Bajt, Atomic hydrogen cleaning of EUV multilayer optics, this SPIE Proc. (2003).

21. M. Singh, and J. J. M. Braat, Capping layers for extreme-ultraviolet multilayer interference coatings, *Opt. Lett.* **26**, 259-261 (2001).

22. A.E. Yakshin, E. Louis, E.L.G. Maas, F. Bijkerk, R. Klein, F. Scholze, P. Zalm, F. Stietz, M. Wedowski, S. Muellender, B. Mertens, and H. Meiling, Protection of Mo/Si multilayers with a carbon capping layer, ASET/SEMATECH Workshop on Extreme UV Lithography, Matsue Vol. CD, pp. P6-6 (2001).

23. J. H. Underwood, and E. M. Gullikson, High-resolution, high-flux, user friendly VLS beamline at the ALS for the 50-1300 eV energy region, *J. Electron Spectrosc. Relat. Phenom.* **92**, 265-272 (1998).

24. M. Malinowski, private conversation.
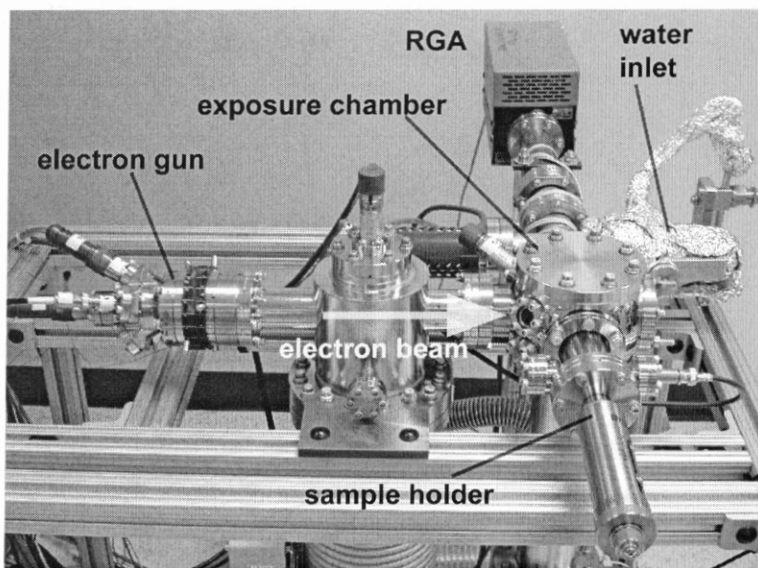
25. R. Hudyma,

26. D. O'Connell

Figure 1: A photo of the electron beam chamber at Sandia National Laboratory, which was used for electron beam exposures.
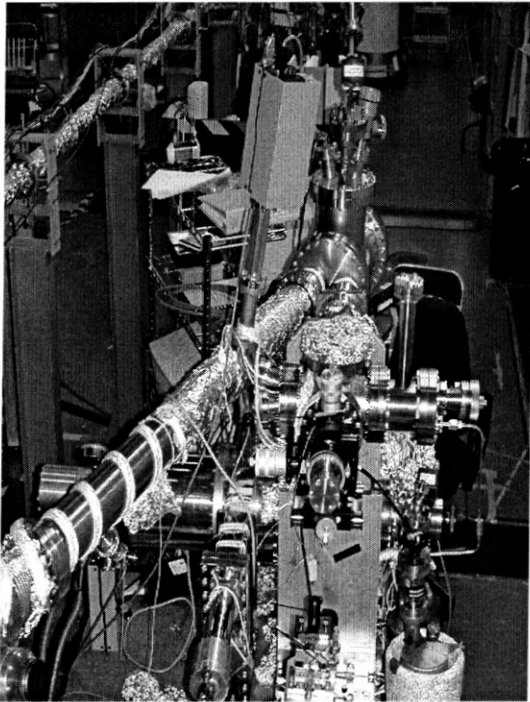
Figure 2: A photo of the NIST environmental chamber used for EUV light exposures.
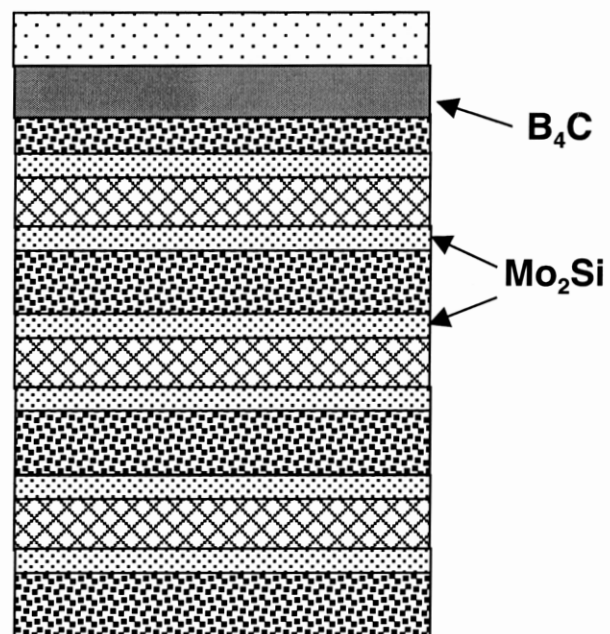

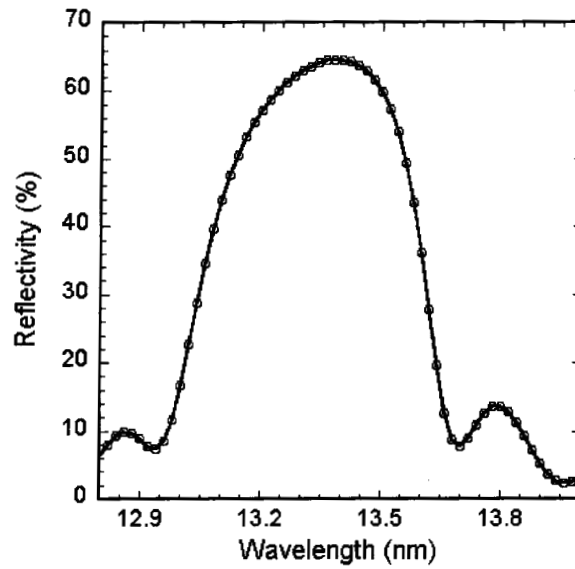Figure 3: Schematic view of capping layer design and the multilayer in this study.

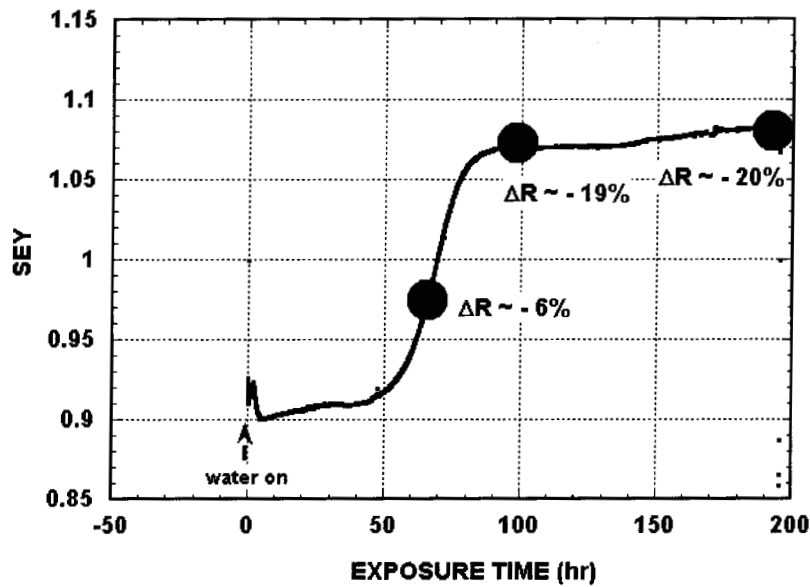Figure 4: Reflectivity as a function of wavelength of a Ru-capped multilayer.

Figure 5: Secondary electron yield (SEY) emission as a function of exposure time shows a sudden increase after ~50 hours of electron beam exposure in water vapor environment. Shown here is also reflectance drop (absolute values) as a function of the exposure time.
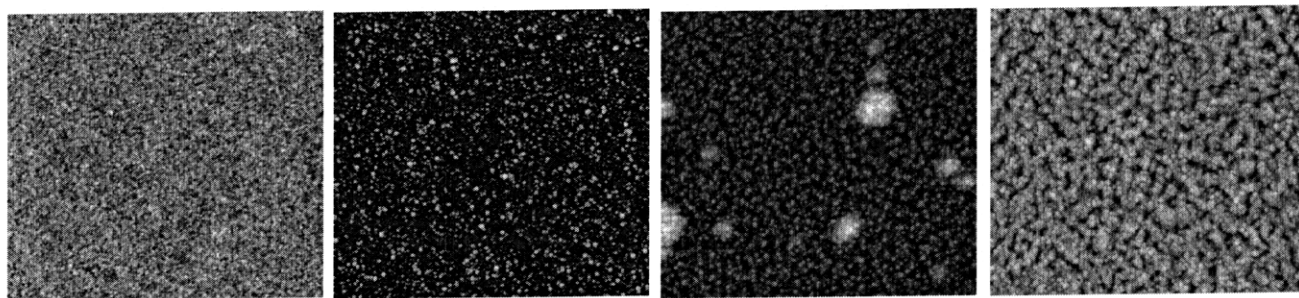
Figure 6: Two dimensional AFM scans (2 x 2 _m) on a Ru-capped multilayer on an unexposed area (a), on the area exposed to 60 hours (b), 100 hours (c) and ~200 hours (d). The measured RMS surface roughness: 0.19 nm (a), 1.19 nm (b), 2.87 nm (c) and 1.65 nm (d).
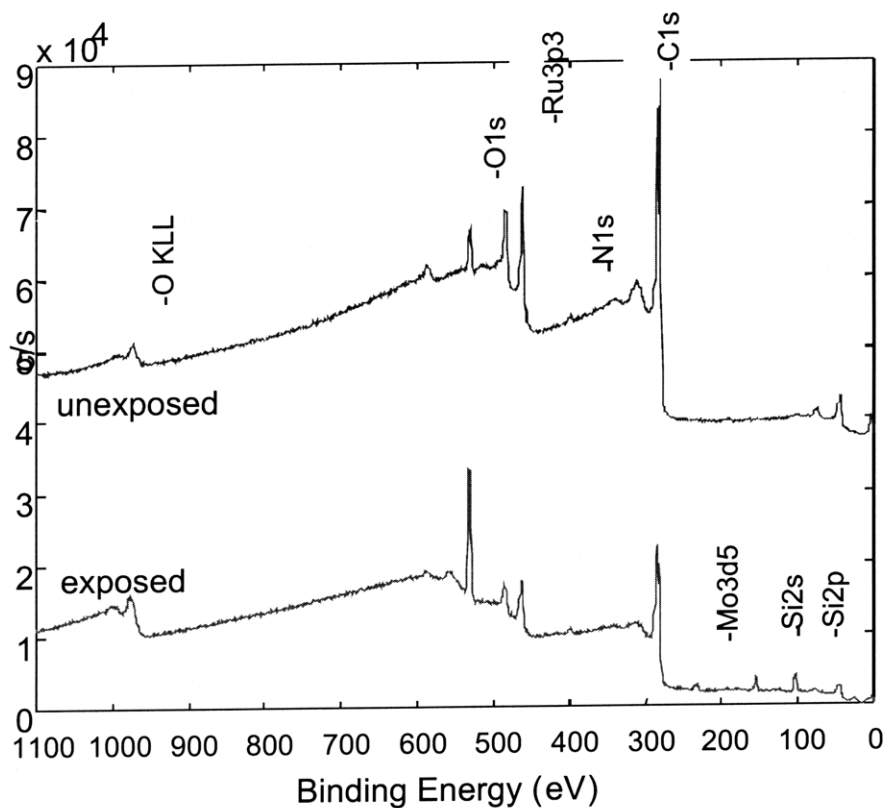

Figure 7: XPS spectra of unexposed Ru-capped multilayer and of Ru-capped multilayer that was exposed to the electron beam in the presence of water vapor for 100 hours.
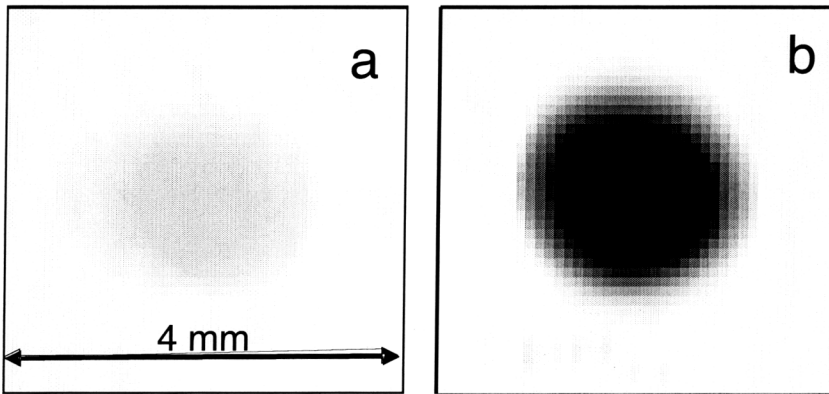
Figure 8: Reflectance maps on Ru-capped multilayer (a) and Si-capped multilayer (b) after ~60 hours of electron beam exposure in water vapor environment. The greyscale is the same for both maps and ranges on a linear scale from −17% (black) to 0% (white).
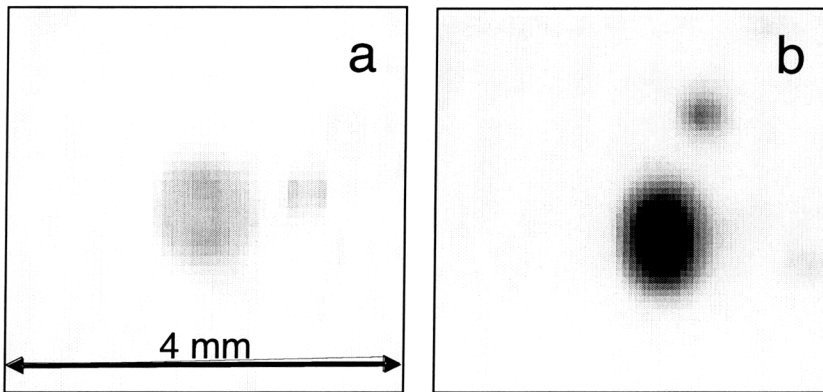

Figure 9: Reflectance maps on Ru-capped multilayer (a) and Si-capped multilayer (b) after ~60 hours of EUV beam exposure in water vapor environment. The greyscale is the same for both maps and ranges on a linear scale from −16.5% (black) to 0% (white).

Table 1: Lifetime calculations based on electron beam extrapolations (L_{e^-}) and EUV beam extrapolations (L_{EUV}). The lifetimes based on electron beam extrapolations are the lower limit values.

	Area (cm^2)	P (mW/cm^2)	L_{e^-} (years)	L_{EUV} (years)
Mask	161	43.3	0.15	0.12
M1	127	17.5	0.4	0.3
M2	162	8.7	0.7	0.6
M3	78	11.1	0.6	0.5
M4	495	1.0	6.4	5.6
M5	39	7.5	0.9	0.7
M6	536	0.3	21.4	18.5